UNITED NATIONS EDUCATIONAL, SCIENTIFIC AND CULTURAL ORGANIZATION
INTERNATIONAL ATOMIC ENERGY AGENCY
INTERNATIONAL CENTRE FOR THEORETICAL PHYSICS
I.C.T.P., P.O. BOX 586, 34100 TRIESTE, ITALY, CABLE: CENTRATOM TRIESTE

SMR/1006 - 9

COURSE ON "OCEAN-ATMOSPHERE INTERACTIONS IN THE TROPICS"
26 May - 6 June 1997

"The Seasonal Cycle in a Coupled Ocean-Atmosphere Model"

presented by

P. CHANG
Physical Oceanography
Texas A&M University
College Station, TX
USA

Please note: These are preliminary notes intended for internal distribution only.

Reprinted from JOURNAL OF CLIMATE, Vol. 7, No. 8, August 1994
American Meteorological Society

The Seasonal Cycle in a Coupled Ocean–Atmosphere Model

BENJAMIN S. GIESE AND JAMES A. CARTON

The Seasonal Cycle in a Coupled Ocean–Atmosphere Model

BENJAMIN S. GIESE AND JAMES A. CARTON

Department of Meteorology, University of Maryland, College Park, Maryland

(Manuscript received 23 March 1993, in final form 23 August 1993)

ABSTRACT

A coupled ocean–atmosphere model is used to investigate the seasonal cycle of sea surface temperature and wind stress in the Tropics. A control run is presented that gives a realistic annual cycle with a cold tongue in the eastern Pacific and Atlantic Oceans. In an attempt to isolate the mechanisms responsible for the particular annual cycle that is observed, the authors conducted a series of numerical experiments in which they alter the solar forcing. These experiments include changing the longitude of perihelion, increasing the heat capacity of land, and changing the length of the solar year. The results demonstrate that the date of perihelion and land heating do not, by themselves, control the annual cycle. However, there is a natural timescale for the development of the annual cycle. When the solar year is shortened to just 6 months, the seasonal variations of climate remain similar in timing to the control run except that they are weaker. When the solar year is lengthened to 18 months, surface temperature in the eastern Pacific develops a prominent semiannual cycle. The semiannual cycle results from the ITCZ crossing the equator into the Southern Hemisphere and the development of a Northern Hemisphere cold tongue during northern winter. The meridional winds maintain an annual cycle, while the zonal winds have a semiannual component. The Atlantic maintains an annual cycle in all variables regardless of changes in the length of the solar year. A final experiment addresses the factors determining the season in which upwelling occurs. In this experiment the sun is maintained perpetually over the equator (simulating March or September conditions). In this case the atmosphere and ocean move toward September conditions, with a Southern Hemisphere cold tongue and convection north of the equator.

1. Introduction

The Pacific, Atlantic, and Indian Oceans all have pronounced annual cycles of SST (sea surface temperature) and wind stress in the Tropics. A succinct description of the annual cycle of the Pacific Ocean–atmosphere system has existed for over a decade (Horel 1982). In the North Pacific extratropics SST is warmest in late northern summer and, likewise, SST in the Southern Hemisphere is warmest during southern summer. This merely reflects the considerable impact of insolation on extratropical SST. In the equatorial central and eastern Pacific, however, the phase of the annual cycle of SST does not reflect the path of the sun. There is a noticeable delay in seasonal warming moving westward from the coast of South America along the equator. Horel (1982) interprets this delay as evidence that oceanic Rossby waves play an important role in the evolution of the seasonal cycle of SST in the tropical Pacific.

If the midlatitude argument that warm SST responds to changes in the declination of the solar angle is extended to the equatorial region, one could naively expect SST variability to be dominated by a semiannual cycle, because the sun is directly overhead not once but twice per year. However, observations of SST at the equator reveal that the cycle of SST variations is not semiannual, but annual, and coincides with the annual migration of the intertropical convergence zone (ITCZ). SST is warmest on the equator when the ITCZ is closest to the equator, during the months of March, April, and May and is coldest when the ITCZ is farthest north, during July through September.

Horel has also documented the annual variations in surface winds (and in the associated divergence). While there is a well-defined annual cycle in meridional winds across all longitudes, the annual cycle amplitude is more pronounced along the western and eastern coasts. The annual cycle in surface divergence is particularly large in the central and eastern Pacific and is unquestionably linked to surface meridional wind variability there. Due to the presence of a pronounced annual cycle in both SST and surface winds (mostly the meridional component), the ocean and the atmosphere are likely strongly coupled in the tropical eastern Pacific.

Mitchell and Wallace (1992) argue for the importance of the monsoonal circulation driven by heating of the Central American landmass in initiating the seasonal northward flow in the northern Tropics beginning in June and intensifying in the subsequent months. This northward flow, they argue, generates a region of colder SST just south of the equator that, through

Corresponding author address: Dr. Benjamin S. Giese, Department of Oceanography, Texas A&M University, College Station, TX 77843.

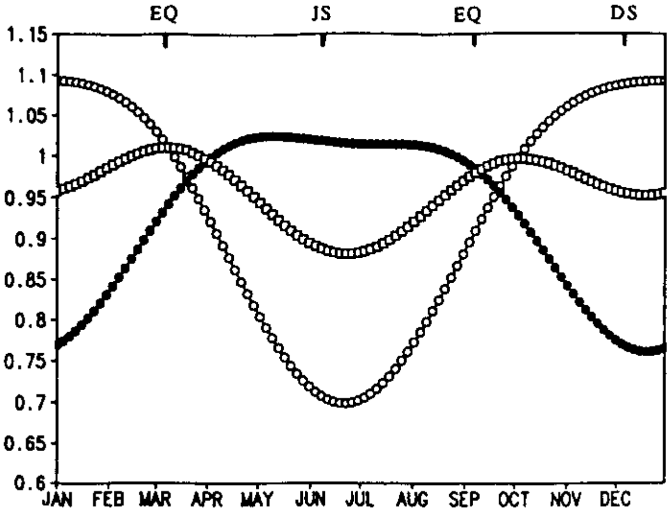

FIG. 1. Solar forcing as a function of time of year for the equator (squares), 15°N (closed circles), and 15°S (open circles). The time of the June solstice (JS), December solstice (DS), and the two equinoxes (EQ) are shown on the upper axis.

planetary boundary layer cooling, increases the sea level pressure (Lindzen and Nigam 1987). Increased sea level pressure results in more northward and westward flow, which is postulated to yield even colder temperatures, resulting in a positive feedback mechanism. A month-by-month description of the departures from the annual mean conditions (e.g., see Halpert and Ropelewski 1989) indicates that the northeastward flow in the northern Tropics of the eastern Pacific begins as an onshore flow into Panama in Central America and develops in amplitude and westward extent with the progression of the seasons. Mitchell and Wallace have also shown that this flow occurs simultaneously (or with some lead) with respect to the annual cycle of SST.

First consider the temporal and spatial variations of solar radiation at the top of the atmosphere. Insolation on the equator, at 15°N and 15°S, is shown in Fig. 1. On the equator, insolation is largest during the vernal and autumnal equinoxes, when the sun is directly overhead. During the solstices solar radiation reaches its minimum value, with insolation during the June solstice noticeably less than during the December solstice. The difference in insolation between the solstices is because perihelion, marking the earth's closest approach to the sun, occurs in early January, and aphelion occurs in early July. Thus, there are two components of solar radiation on the equator: a semiannual cycle due to the declination of the earth's axis of rotation and an annual cycle due to the ellipticity of the earth's orbit around the sun.

At 15°S, solar radiation has a dominant annual cycle, with the December solstice coinciding with perihelion. Since insolation in the Southern Hemisphere is least during the June solstice, and the June solstice coincides with aphelion, the range between the largest value of solar radiation and the smallest value of radiation at 15°S is greater than the range at 15°N. At 15°N the cycle of radiation is also strongly annual, with a slight dip in radiation during the June solstice because of decreasing insolation associated with aphelion. Thus, in the extratropics annual forcing is composed of the effect of both the earth–sun distance and the earth's declination.

Despite the dominance of semiannual solar forcing on the equator, observations of the tropical oceans show that the Pacific and Atlantic Oceans have dominant annual cycles. Observations show that the eastern Pacific has a cold tongue of water that extends from the coast of South America to 120°W from mid-June through February (Fig. 2a). The cold tongue is replaced by warm water for a shorter period of time, from March through May, before the cold tongue reappears. The Atlantic has a similar cycle, except that it extends across the entire Atlantic basin, and the cold period does not last as long. The observations also show that the Indian Ocean has a weak annual cycle, with its largest variation confined to the western part of the basin.

Zonal wind stress (Fig. 2b) shows the presence of easterlies across the Pacific and Atlantic basins, with

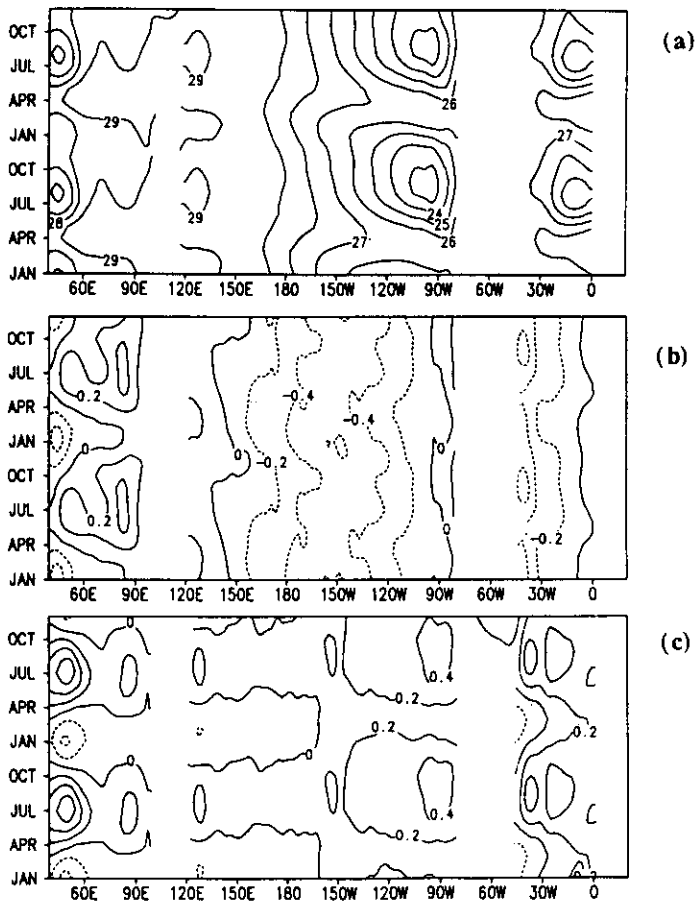

FIG. 2. (a) Observed monthly averaged equatorial SST (°C) for the period 1982–92. Monthly means of (b) zonal wind stress (dyn cm^{-2}) and (c) meridional wind stress (dyn cm^{-2}) based on Hellerman and Rosenstein (1983).

westerlies near the continental margins in the eastern Atlantic and Pacific and in the western Pacific. The Indian Ocean has prominent westerlies in the eastern part of the basin, with annually reversing zonal wind stress in the western Indian Ocean. Meridional wind stress, shown in Fig. 2c, has northerly flow across the equator in the eastern part of the Atlantic and Pacific basins and has flow across the equator in both directions in the western Atlantic and Pacific basins. The Indian Ocean has strong meridional winds that change direction across the equator in the western Indian Ocean, with weakly reversing winds in the eastern Indian Ocean.

In this paper we attempt to answer the question, Why do the equatorial oceans have a pronounced annual cycle, when the dominant source of solar forcing on the equator is semiannual? This question is intrinsically linked to the question, Why does the ITCZ reside almost exclusively in the Northern Hemisphere? To address this question, we explore three hypotheses. The first hypothesis is that the annual cycle of perihelion–aphelion forces the ocean annual cycle. The second hypothesis is that the annual cycle of land heating forces the ocean annual cycle, and the third hypothesis is that a resonant response of the oceans to forcing near a 12-month period is responsible for the dominant annual cycle in the oceans. Our approach is to use a coupled ocean–atmosphere model that gives a realistic representation of the seasonal cycle and to test the hypotheses by means of a series of numerical experiments. Section 2 describes the model and the numerical experiments, and a summary and conclusions are presented in section 3.

2. Model experiments

The atmospheric component of the coupled model is an R15 spectral model with 18 vertical levels and is described in detail by Kinter et al. (1988). The parameterization of moist processes includes a modified Kuo scheme for moist deep convection (Sela 1980), a shallow convective mixing scheme, and large-scale condensation. Radiative transfer is calculated according to the Lacis and Hansen (1974) scheme for short wavelengths and according to the Harshvardhan et al. (1987) scheme for long wavelengths. The distribution of cloudiness required by the radiative calculations is internally calculated following Slingo (1987).

The model includes crude parameterizations of near-surface processes. Tendencies due to vertical transport of heat, water vapor, and momentum in the planetary boundary layer are ascribed to two processes: small-scale turbulence and shallow moist convection. The tendency due to each of these processes is assumed to be given by vertical diffusion with separately calculated coefficients.

At each time step, the level 2 closure scheme of Mellor and Yamada (1982) is applied to find the diffusion coefficients for heat, moisture, and momentum due to dry turbulence. The Mellor–Yamada scheme helps produce a realistic diurnal cycle of the planetary boundary layer over land in the model.

When the atmosphere is unstable to moist convection but does not satisfy the criterion for deep-precipitating convection, vertical diffusion of heat and moisture is applied between cloud base and cloud top to simulate the effects of shallow nonprecipitating moist convection (Tiedtke 1983). After the moist convection parameterization is applied, the atmosphere is tested for supersaturation. If supersaturation is found, a wet-bulb adjustment is applied to reduce the atmosphere to saturation and the excess moisture precipitates out, evaporating if the layers through which it falls are unsaturated.

The transfer of heat, moisture, and momentum from the surface to the atmosphere are parameterized using bulk formulas, with the transfer coefficients found as a function of the Richardson number using the dimensional analysis method of Monin and Obukhov (1954).

The ocean component of the coupled model is a medium-resolution version of the MOM (modular ocean model) code developed at the National Oceanic and Atmospheric Administration's Geophysical Fluid Dynamics Laboratory (Pacanowski et al. 1991). The version used here is global in extent, with 240 grid points in longitude, giving a zonal resolution of 1.5°. There are 123 grid points in latitude spanning from 70°S to 65°N. The grid spacing is variable in latitude, with constant resolution of 0.5° from 10°S to 10°N and increasing poleward of 10° to a maximum of 1.5°. The grid spacing also varies as a function of depth, with 10 out of a total of 16 vertical levels in the upper 300 m. A realistic bathymetry is used, with depths interpolated from the Scripps 1° by 1° topography. Major islands are included in the basin geometry.

The model employs a Richardson number–dependent mixing scheme, as in the hindcast experiments of Philander and Seigel (1985). Horizontal mixing is calculated along isopycnal surfaces, using a coefficient of mixing that depends nonlinearly on the horizontal scales of the flow. The surface flux of heat and momentum is determined by the atmosphere, so that the coupled model is internally consistent in that energy is not lost or gained in the system over time.

The coupling proceeds as follows: The atmosphere is started from observed SST conditions and integrated forward for three model hours. The resulting wind stress and heat fluxes are passed to the ocean, which is started from rest with Levitus (1982) temperature and salinity fields. The ocean is integrated forward for three hours, and SST is given back to the atmosphere, thus completing the cycle. The coupled model is spun up for one year, giving the initial state for the following experiments.

a. The annual cycle of SST and wind

The first experiment described is a control run, integrated for 7 years. To construct monthly means, averages were taken over the last 5 years of the experiment. Model monthly mean SST is shown in Fig. 3a for the control run. The major features of the observed annual cycle are captured by the coupled model. The eastern Pacific has a well-defined annual cycle, with a minimum temperature of about 25°C. The cool period in the eastern Pacific lasts for about 9 months and is followed by a period of about 3 months when SST warms to 27°C. The western Pacific consists of warm water with a temperature of just over 30°C and does not have a well-defined annual cycle, in agreement with the observations. There is a weak semiannual cycle of SST in the western Pacific in both the model and the observations. The strength of the semiannual cycle in the western basins results from the relative uniformity of SST. Under those conditions, changes in solar radiation, which has a semiannual cycle, seem to determine SST.

There are, however, notable differences between the control model SST field (Fig. 3a) and the observed field (Fig. 2a). The model is too warm in the far eastern Pacific, with water that exceeds 28°C adjacent to the coast of South America. There is evidence that this warm water is the result of too little marine stratus in the atmosphere model so that there is unrealistically high insolation in the eastern Pacific and eastern Atlantic Oceans (Z. Zhu 1992, personal communication). The modeled cold tongue is 2°C warmer than observed; this is undoubtedly caused by zonal wind stress that is too weak (Fig. 3b). Another consequence of weak zonal winds is that the simulated longitudinal SST gradient is too weak in the eastern Pacific and too strong in the western Pacific, with SST varying from 27°C near the date line to over 30°C at 120°E. The observations show little SST variation in this region.

The model annual cycle in the Atlantic also shows similarities as well as differences with the observed annual cycle. Although the timing and basic patterns of the annual cycle in the model Atlantic basin resemble observations, the annual cycle in the model is too weak, with a minimum temperature of 26°C, as compared with an observed minimum of 25°C. SST is too warm along the coast of Africa; again, this is probably due to problems in resolving clouds. The Indian Ocean model results compare least favorably with observations, with a strong annual cycle of SST in the eastern Indian Ocean. Zonal wind stress in the model is primarily easterly, whereas observations show westerly winds on the equator. This large difference between modeled and observed winds is the result of a northward shift of the trade wind system.

Model meridional wind stress, shown in Fig. 3c, shows a strong annual cycle in all three basins. Consistent with observations wind stress is predominantly southerly in the eastern Pacific and weakens simultaneously with the warming of SST. However, the model winds in the central Pacific show a seasonal reversal in direction. The observations (Fig. 2c) show that the region of reversing winds is confined to west of the date line. In the Atlantic and Indian Oceans simulated meridional wind stress is similar to the observations.

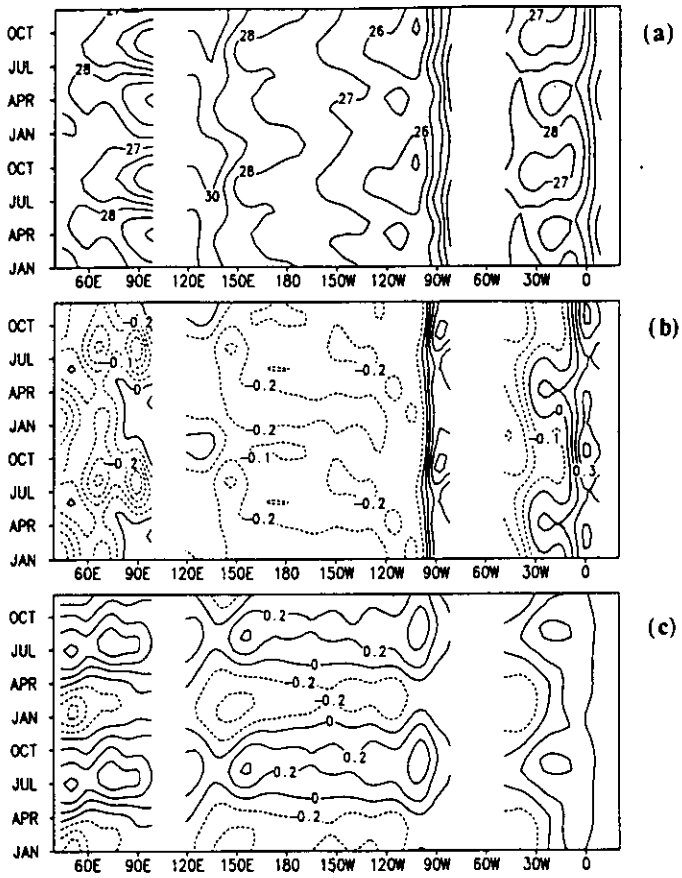

FIG. 3. Time-longitude contour from the control run of (a) SST (°C), (b) zonal wind stress (dyn cm^{-2}), and (c) meridional wind stress (dyn cm^{-2}).

The annual cycle of SST and zonal wind stress is too weak, whereas the annual cycle of meridional wind stress is about the same as observed. This seems to result from difficulties that the atmospheric model has in producing a realistically strong ITCZ. We speculate that the R15 resolution is inadequate to allow the distinct region of reduced wind speed that is observed. Thus, as the model ITCZ shifts seasonally, the zonal equatorial trade winds have less seasonal variation than they should. The meridional winds are determined by the large-scale Hadly circulation and are better resolved by the R15 model.

b. Perihelion and the annual cycle

To test the hypothesis that the annual cycle of the earth–sun distance causes the annual cycle of SST in the tropical oceans, an experiment was conducted whereby the phase of perihelion was artificially changed

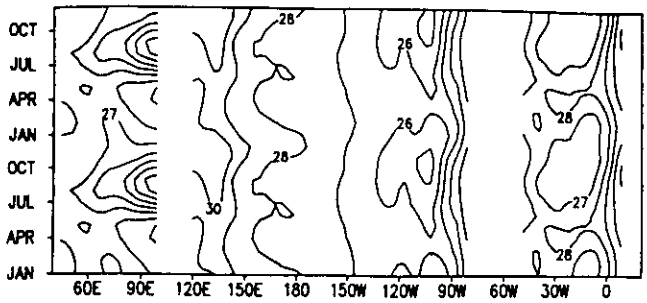

FIG. 4. Monthly mean SST (°C) from the experiment where perihelion occurs in July.

so that perihelion occurs in early July, keeping all other aspects of the model integration the same as in the control case. These orbital parameters are similar to those of the earth 18 000 years before present. The perihelion experiment was integrated for 5 years, with initial conditions provided from the control run at year 2. The last 4 years are used in calculating monthly means. If the hypothesis that perihelion controls the annual cycle is correct, then the equatorial cold tongue should weaken during northern summer because of enhanced solar radiation.

Model monthly mean SST from this experiment is presented in Fig. 4. With perihelion in July, SST in the eastern tropical Pacific and in the Atlantic is about 0.5°C cooler than in the control case. With solar forcing slightly larger during northern summer, the southeast trades become stronger, leading to increased upwelling on the equator. This is the opposite of the anticipated result that the equatorial cold tongue would weaken by having perihelion in July. Instead of the time of perihelion explaining the existence of the equatorial annual cycle, altered dynamics act to weaken the annual cycle.

c. Land heating and heat capacity

A second hypothesis is that land-surface heating plays a crucial role in the development of the annual cycle. Since the effective heat capacity of land is much lower than that of ocean, land heats up and cools off more quickly. To test the hypothesis that differential heating caused by a greater percentage of land in the Northern Hemisphere controls the development of the annual cycle, an experiment was conducted in which the heat capacity of land was artificially increased by a factor of 60 [North et al. (1983) use a land heat capacity that is a factor of 60 less than that of the ocean] so that it more closely resembles that of the ocean. The high–heat capacity experiment was run for 5 years, with monthly mean values based on the final 4 years of integration. Except for the change to land and vegetation heat capacity, this experiment is identical to the control case.

The effect of increased land heat capacity on surface temperature averaged from the equator to 45°N is shown in Fig. 5a. In the control case, Northern Hemisphere surface temperature ranges from a minimum of about 18°C in January to a maximum of 27.5°C in August, giving an annual range of temperature of 9.5°C. In the high–heat capacity experiment, Northern Hemisphere surface temperature varies from about 20.5°C in February to 24°C in August, giving an annual range of 3.5°C. The Southern Hemisphere, which has a much larger percentage of surface area covered with ocean, shows a much smaller change in surface temperature between the two cases. In the control case surface temperature in the Southern Hemisphere varies from just over 21°C in July to a maximum in February of just over 27°C, resulting in an annual range of 6°C. Since there is some land south of the equator, increasing the heat capacity results in a small change of surface temperature. In the high heat capacity case, surface

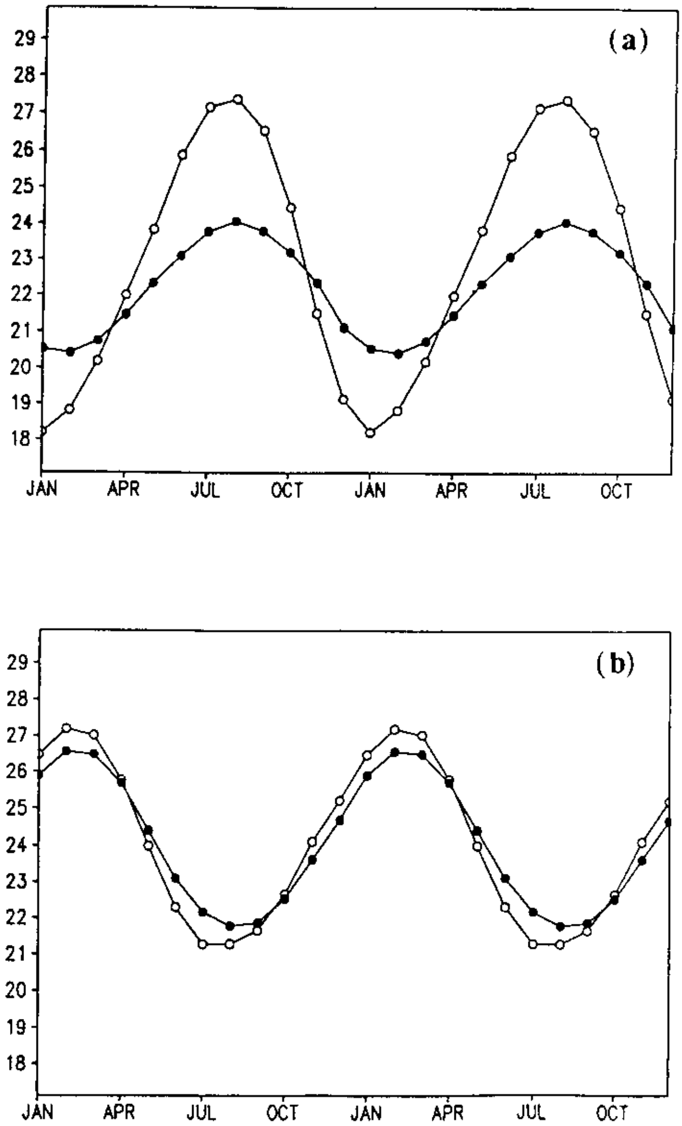

FIG. 5. Surface temperature (°C) averaged from (a) the equator to 45°N and (b) the equator to 45°S. The control case is shown with open circles and the high–heat capacity experiment is shown with closed circles.

temperature has a range of 4.5°C, from about 22°C in August to 26.5°C in February. The similarity between the two hemispheres in the high-heat capacity case indicates that land and ocean have approximately the same overall heat capacities.

Monthly mean SST from the high-heat capacity case is shown in Fig. 6. The high-heat capacity experiment shows that the annual cycle is altered by changing the land heating, but there is still a dominant annual cycle. In the central Pacific there is a prominent semiannual cycle of SST; otherwise, SST is similar to the control case. Eliminating the difference between land and ocean surface heating does not significantly alter the annual cycle.

d. Varying the length of the solar year

With a coupled model of the Tropics, we are able to vary some free parameter of the system and investigate how the coupled system responds to the change. In the coupled ocean–atmosphere system, forcing ultimately comes from the seasonally varying solar radiation. Therefore, experiments have been conducted that examine the response of the coupled ocean–atmosphere system to variations in the period of solar forcing. As a control run the same annual cycle described before is used. The frequency of forcing is then varied, so that the length of the solar year is 6 months in one case and 18 months in the other. The 6-month year experiment was integrated for 9 cycles, and the last 5 cycles are used for the monthly means. Because of the long period, the 18-month year case was integrated for only 4.5 cycles, the last three of which were used in calculating the monthly means.

In the 6-month year case, variations of SST on the equator are weak in both the Pacific and Atlantic basins (Fig. 7a). The seasonal cycle of SST in the eastern Pacific is much weaker than in the 12-month case, with temperature variations of only about 1°C from the peak of the cool period to the peak of the warm period. The seasonal cycle of SST in the Atlantic is also much weaker, with a brief cooling to just below 27°C that occurs in the central Atlantic. The 6-month case is, to first approximation, a weaker version of the 12-month

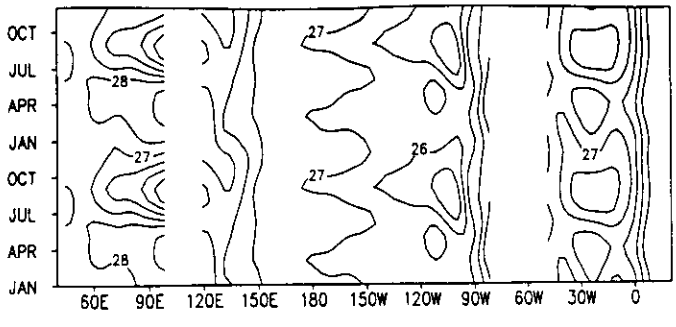

FIG. 6. Monthly mean SST (°C) from the experiment with high-land heat capacity.

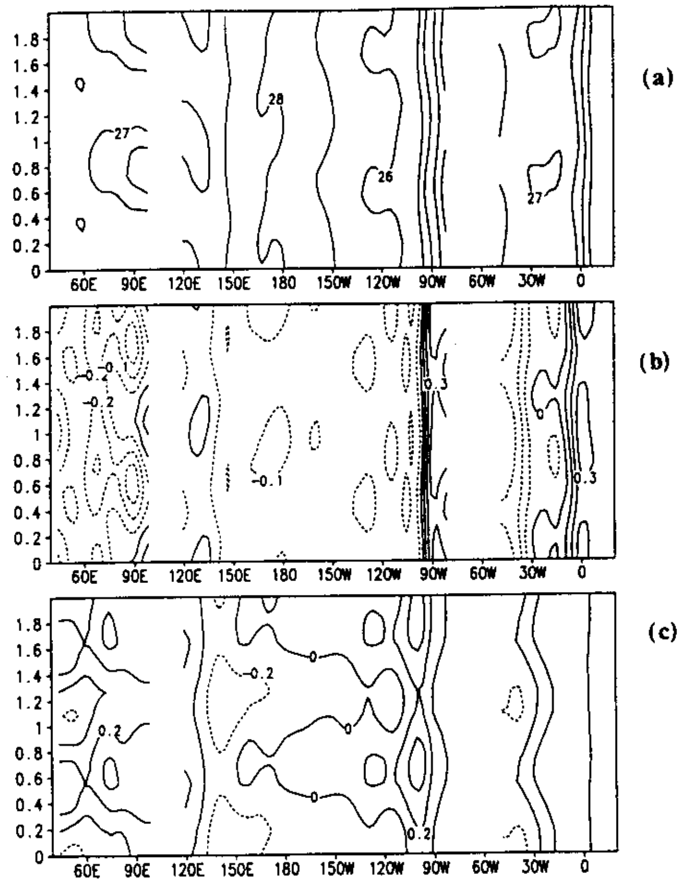

FIG. 7. Time–longitude contour from the 6-month year run of (a) SST (°C), (b) zonal wind stress (dyn cm^{-2}), and (c) meridional wind stress (dyn cm^{-2}). The vertical axis represents two cycles of the run with time 0, the same time as 15 January of the solar cycle.

year case. The zonal winds are weak in the 6-month year (see Fig. 7b), showing almost no variation when contoured using the same interval as in the 12-month year. The weak zonal winds are consistent with the weak zonal SST gradient.

While the 6-month case resembles a weakened version of the control case, the 18-month case shows an interesting combination of similarities and marked contrasts with the control case. In the Atlantic Ocean, SST has an annual cycle, as in the control case. The annual cycle is stronger in the 18-month case, with a range in the Atlantic of 25°C during the cold season to 30°C at the peak of the warm season.

The Pacific Ocean, on the other hand, behaves very differently in the 18-month case than in the control. SST in the equatorial Pacific develops a prominent semiannual cycle, with two cold tongues developing in a single solar year. The more intense cold tongue in Fig. 8a is associated with the usual development of cold water in the tropical Pacific. It forms when the southeast trades intensify and cold water extends from the coast of South America onto the equator. What is unusual in this experiment is that a northern cold tongue develops in northern winter, so that the eastern Pacific experiences cool SST while the Atlantic Ocean

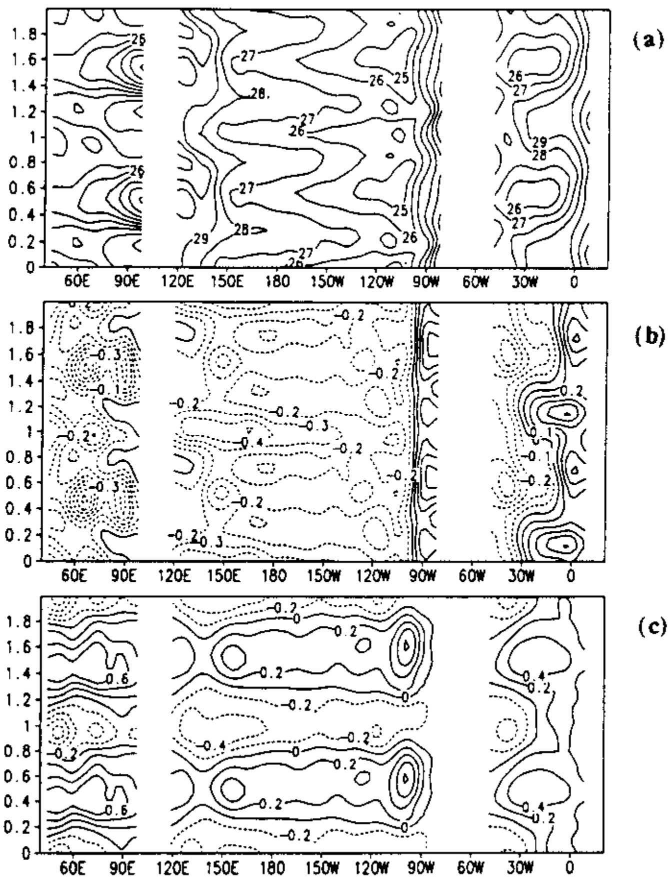

FIG. 8. As in Fig. 7 but for the 18-month case.

has its warmest SST. This cooling is weaker than the cooling that occurs in northern summer.

The meridional winds, shown in Fig. 8c, demonstrate that there is an increase in cross-equatorial flow, consistent with the development of a Southern Hemisphere ITCZ. Interestingly, however, the meridional winds do not have a semiannual cycle as in SST, but maintain an annual cycle as in the control case. The zonal wind component does have a semiannual cycle, showing a relaxation of the trades twice per 18-month year.

A vivid demonstration of how the eastern Pacific makes the transition from being dominated by the annual cycle to being dominated by a semiannual cycle is shown in Fig. 9, where heat content for the three experiments is shown as function of longitude and time. Heat content in the 6-month case shows a weak annual cycle with no evidence of a semiannual cycle. The control case, shown in Fig. 9b, shows that heat content in the western Pacific has contributions from both the semiannual and annual cycle, consistent with the ITCZ crossing the equator in the western Pacific. In the eastern Pacific heat content is dominated by an annual cycle, although it is not particularly strong. In the 18-month case heat content in the Pacific is strongly semiannual across the basin. These semiannual variations in heat content result from fluctuations in thermocline depth and are associated with the semiannual variation in SST.

e. Perpetual March solar radiation

Experiments varying the length of the solar year have shown that a 12-month solar cycle is too short to warm up each summer hemisphere sufficiently to cause the ITCZ to shift hemispheres, but remaining unexplained is why present-day climate has the ITCZ in the Northern Hemisphere. In a final experiment the sun was fixed permanently over the equator, so that there is no seasonal variation in insolation. The time-averaged ocean response to such forcing is shown in Fig. 10, along with the SST pattern for monthly mean March and September conditions from the control case. SST in the perpetual March case shows a distinct asymmetry between the Northern and Southern Hemispheres. This asymmetry is manifested by a semipermanent pool of warm water located off the coast of Costa Rica (the Costa Rica Dome), whereas cool water extends from the southern extratropics near the coast of South America all the way to the equator. The stationary state, with a pronounced cold tongue, is closer to conditions in September than the conditions in March. A similar mean state is apparent in the study of Philander et al. (1992). In their study with time mean solar forcing, SST is more similar to September conditions than to March conditions.

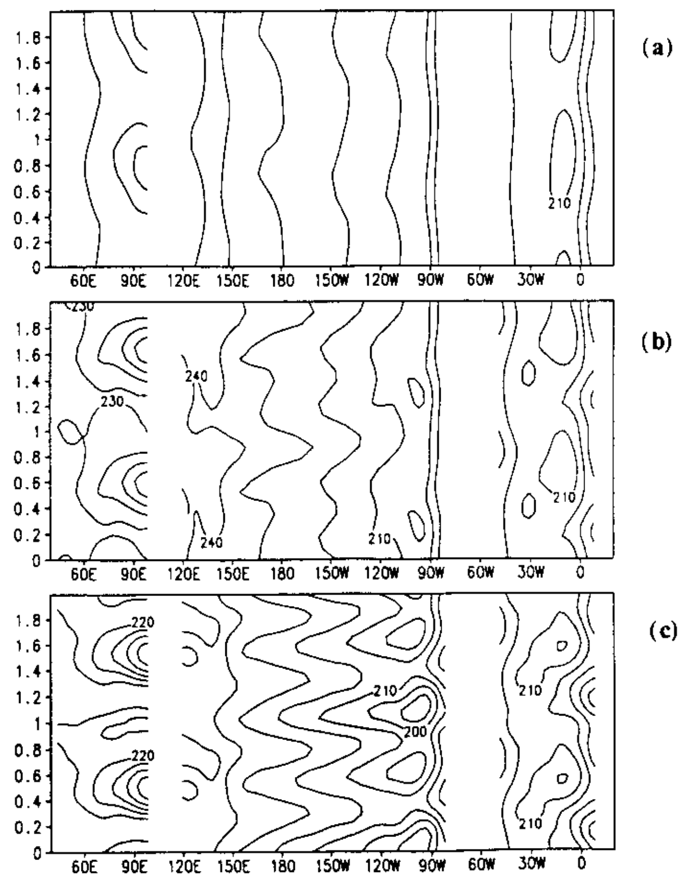

FIG. 9. Time–longitude contours of temperature integrated to a depth of 350 m for (a) the 6-month year, (b) the 12-month year, and (c) the 18-month year experiment.

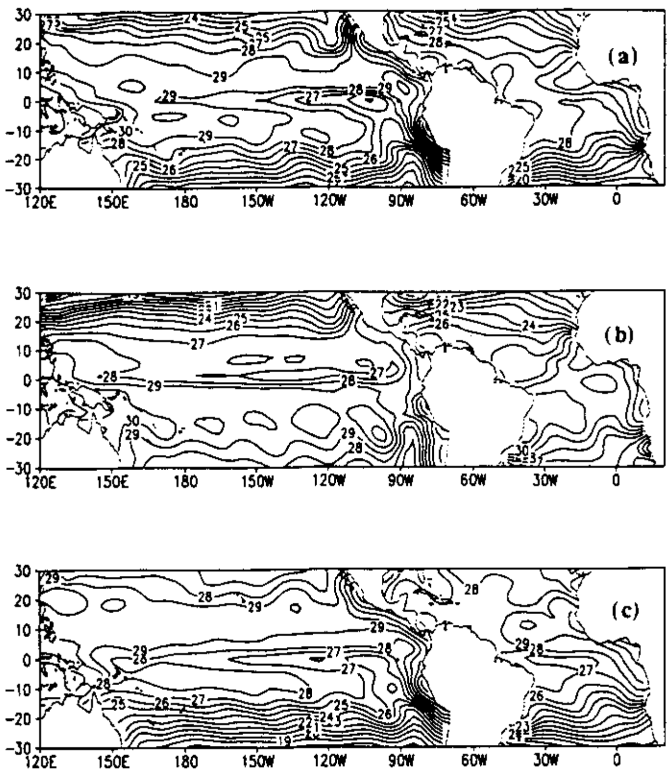

FIG. 10. SST (°C) for (a) perpetual equinox solar forcing, (b) monthly mean March conditions from the control run, and (c) monthly mean September conditions from the control run.

By adding a seasonal component of solar forcing to this steady solution, it becomes clear why the equator responds annually to semiannual forcing. For the ocean to have a semiannual cycle, cool water south of the equator in the eastern Pacific must be warmed sufficiently so that the ITCZ can cross into the Southern Hemisphere. Since this process is slow, cold water adjacent to the coast of South America is never warmed sufficiently for the ITCZ to cross into the Southern Hemisphere. The inherent asymmetry in the steady case forces the ITCZ to remain in the Northern Hemisphere, thus providing annual forcing of the equatorial zone.

When the length of the solar year is decreased to 6 months, the steady solution dominates over the seasonal part, and so the seasonal cycle becomes weak. In the eastern Pacific this means that northward cross-equatorial flow persists, while in the western Pacific there is a weak annual cycle of meridional winds.

As the length of the year increases, first to 12 months and then to 18 months, the region of seasonally reversing meridional winds moves from the western Pacific into the central and eastern Pacific. This cross-equatorial flow represents an annual shift of the ITCZ into the Southern Hemisphere. When the length of the year is increased to 18 months, the equatorial response is qualitatively different from the control run. In the 18-month case the ITCZ does cross the equator so that a Northern Hemisphere cold tongue develops during northern winter.

3. Summary and conclusions

Despite the dominance of semiannual solar forcing on the equator, observations of the tropical oceans show that the Pacific and Atlantic Oceans have dominant annual cycles. In this paper we attempt to answer the question, Why do the equatorial oceans have a pronounced annual cycle when the dominant source of solar forcing on the equator is semiannual? This question is the same as asking why the ITCZ resides north of the equator throughout the year in much of the Tropics. The annual cycle of the Tropics is fundamentally the result of coupled interactions of the ocean–atmosphere system, and questions such as this cannot be addressed solely in terms of the atmosphere or ocean.

First a control run is presented that demonstrates that the coupled model gives a realistic annual cycle. There is an annually occurring cold tongue in the eastern Pacific and Atlantic Oceans that lasts from June through January. The cold tongue is replaced by warm water during March through May. The eastern Indian Ocean also has a strong annual cycle, a feature that is not present in the observations. Zonal wind stress is too weak on the equator, although meridional wind stress has realistic amplitude.

To explore the physical mechanisms responsible for the annual cycle of the Tropics, we test the following three hypotheses: 1) the annual cycle of earth–sun distance forces the annual cycle of SST on the equator, 2) land heating (primarily in the Northern Hemisphere) controls the annual cycle, and 3) the system has a timescale that allows the annual cycle to be amplified preferentially.

To address the first hypothesis, an experiment was conducted in which 180° was added to the longitude of perihelion, so that perihelion occurs in early July instead of early January. Instead of the expected result that the cold tongue weakens during northern summer because of increased solar radiation, the cold tongue strengthens because of intensified trade winds. The increased warming in the Northern Hemisphere causes stronger southeast trade winds across the equator, and so upwelling on the equator intensifies, causing cooler temperatures.

The second hypothesis, that land-surface heating is responsible for the annual cycle, is tested by increasing the heat capacity of land by a factor of 60. Even though the details of the annual cycle are different in the high-heat capacity experiment, the overall annual cycle is similar to the control case. The cold tongue develops at about the same time as in the control, and the minimum temperature is similar as well. The hemispheric distribution of land heating is not, by itself, responsible for determining the annual cycle of the Tropics. To an extent, this result contradicts the Mitchell and Wallace

(1992) hypothesis that monsoonal winds, driven by land heating, give rise to the cold tongue in the eastern Pacific.

The third hypothesis is that the annual cycle exists because of a timescale inherent in the ocean such that oscillations with a 12-month period are preferred over those with a 6-month period. To test this hypothesis, three experiments were run with the coupled model: an experiment with the length of the solar year shortened to 6 months, an experiment with the length of the solar year increased to 18 months, and an experiment using perpetual equinox solar forcing.

When the length of the solar year is reduced to 6 months the seasonal cycle becomes weak. When the length of the solar year is increased to 18 months the seasonal cycle in the Pacific is altered to have a dominant semiannual cycle. The semiannual cycle arises because the ITCZ, which normally resides north of the equator, crosses the equator into the Southern Hemisphere during northern winter as a result of the increase in Southern Hemisphere SST. With the ITCZ in the Southern Hemisphere, a Northern Hemisphere cold tongue develops during northern winter, and so cool water appears on the equator twice per year.

Examination of the results of these experiments indicates that the oceans do introduce a timescale, but one that is determined by the change of SST in response to seasonal changes in winds and heating. For a solar year lasting 12 months, the sun does not remain long enough in the Southern Hemisphere for SST south of the equator to warm sufficiently to cause the ITCZ to shift into the Southern Hemisphere. We are left with the question, Why is northern summer the preferred climate state?

We believe that the asymmetry in the annual cycle results from an asymmetry in the time mean state. In the experiment with perpetual equinox solar forcing a hemispherically asymmetric mean state develops, with a cold tongue that extends out from the coast of South America and onto the equator. By adding an annual component of solar forcing to this steady solution, it becomes clear why the equator responds annually to semiannual forcing. For the pool of warm water located just north of the equator in the eastern Pacific and Atlantic, it is necessary for the ITCZ to cross the equator. This can happen only if the cool water south of the equator in the eastern Pacific is eroded and replaced by warm water, as in the western Pacific. Since this process is slow, there is not enough time for the warm water to extend all the way to the coast of South America, and so the ITCZ never crosses the equator in the eastern Pacific.

The source of the asymmetry that causes the ITCZ to reside primarily in the Northern Hemisphere remains unconfirmed. However, in the course of the present experiments many factors have been ruled out, such as seasonal land heating. Ultimately, the asymmetry must result from the asymmetric distribution of land between the Northern and Southern Hemisphere. One possible mechanism that would explain the asymmetry is that in both the Atlantic and Pacific Oceans the coastline allows the Southern Ocean gyre to extend up to the equator, whereas in the northern oceans, coastal geometry prevents the equatorward advection of cool water in the eastern part of either basin.

These results suggest that it is off-equatorial SST that controls the annual cycle. Previous modeling results (Giese and Cayan 1993) demonstrate that on the equator SST variability is determined by variability of surface wind stress, whereas just off the equator SST variability is dominated by the surface flux of heat. It suggests that the annual cycle on the equator may be controlled by off-equatorial surface fluxes of heat and that the role of equatorial waves may be secondary in importance.

Acknowledgments. Many helpful suggestions on draft copies of the text were provided by S. Nigam and G. Giese and by two anonymous reviewers. The coupled model has been developed by the Center for Coupled Ocean–Land–Atmosphere Interactions under the direction of J. Shukla. This research has been supported by the National Science Foundation (Grant 9000060). Computer time was provided by NCAR.

REFERENCES

Giese, B. S., and D. R. Cayan, 1993: Surface heat flux parameterizations and tropical Pacific sea surface temperature simulations. *J. Geophys. Res.*, **98**, 6979–6989.

Halpert, M. S., and C. F. Ropelewski, 1989: Atlas of tropical sea surface temperature and surface winds. NOAA Atlas No. 8, U.S. Dept. of Commerce, Washington, DC, 13 pp.

Harshvardhan, R. Davis, D. A. Randall, and T. G. Corsetti, 1987: A fast radiation parameterization for general circulation models. *J. Geophys. Res.*, **92**, 1009–1016.

Hellerman, S., and M. Rosenstein, 1983: Normal monthly wind stress over the World Ocean with error estimates. *J. Phys. Oceanogr.*, **13**, 1093–1104.

Horel, J. D., 1982: The annual cycle in the tropical Pacific atmosphere and ocean. *Mon. Wea. Rev.*, **110**, 1863–1878.

Kinter, J. L., J. Shukla, L. Marx, and E. Schneider, 1988: A simulation of the winter and summer circulation with the NMC global spectral model. *J. Atmos. Res.*, **45**, 2486–2522.

Lacis, A. A., and J. E. Hansen, 1974: A parameterization for the absorption of solar radiation in the earth's atmosphere. *J. Atmos. Res.*, **32**, 118–133.

Levitus, S., 1982: *Climatological Atlas of the World Ocean.* NOAA Prof. Paper 13, U.S. Dept. of Commerce, Washington, DC, 173 pp.

Lindzen, R. S., and S. Nigam, 1987: On the role of sea surface temperature gradients in forcing low-level winds and convergence in the tropics. *J. Atmos. Res.*, **44**, 2418–2436.

Mellor, G. L., and T. G. Yamada, 1992: Development of a turbulence closure model for geophysical fluid problems. *Rev. Geophys. Space Phys.*, **20**, 851–875.

Mitchell, T. P., and J. M. Wallace, 1992: On the annual cycle in equatorial convection and sea surface temperature. *J. Climate*, **5**, 1140–1156.

Monin, A. S., and A. M. Obukhov, 1954: Basic laws of turbulent mixing in the ground layer of the atmosphere. *Akad. Nauk SSR, Geofiz. Inst. Tr.*, **151**, 163–187.

North, G., J. Mengel, and D. Short, 1983: Simple energy balance model resolving the seasons and the continents: Application to the astronomical theory of the ice ages. *J. Geophys. Res.*, **88**, 6576–6586.

Pacanowski, R., K. Dixon, and A. Rosati, 1991: The GFDL modular ocean model users guide, version 1.0. Geophysical Fluid Dynamics Laboratory Ocean Group Tech. Rep. 2, 44 pp.

Philander, S. G. H., and A. D. Seigel, 1985: Simulation of El Niño of 1982–1983. *Coupled Ocean-Atmosphere Models*, J. Nihoul, Ed., Elsevier, 517–541.

——, R. C. Pacanowski, N.-C. Lau, and M. J. Nath, 1992: Simulation of ENSO with a global atmospheric GCM coupled to a high-resolution tropical Pacific Ocean GCM. *J. Climate*, **5**, 308–329.

Sela, J. G., 1980: Spectral modeling at the National Meteorological Center. *Mon. Wea. Rev.*, **108**, 1279–1292.

Slingo, J. M., 1987: The development and verification of a cloud prediction scheme for the ECMWF model. *Quart. J. Roy. Meteor. Soc.*, **113**, 899–927.

Tiedtke, M., 1983: The sensitivity of the time mean large scale flow to cumulus convection in the ECMWF model. *Proc. Workshop on Convection in Large Scale Numerical Models*, ECMWF, Reading, United Kingdom, 297–316.